Journal of the European Ceramic Society 22 (2002) 2107–2113

www.elsevier.com/locate/jeurceramsoc

# Microstructure and dielectric characteristics of tungsten bronze structured SBN70 ceramics: effect of $Nb_2O_5$ content

Myoung-Sup Kim[a], Joon-Hyung Lee[a], Jeong-Joo Kim[a,*], Hee Young Lee[b], Sang-Hee Cho[a]

[a]*Department of Inorganic Materials Engineering, Kyungpook National University, Daegu 702-701, Republic of Korea*
[b]*School of Metallurgical and Materials Engineering, Yeungnam University, Kyungsan, Kyungpook 712-749, Republic of Korea*

Received 20 September 2001; received in revised form 17 December 2001; accepted 6 January 2002

**Abstract**

The effect of $Nb_2O_5$ content on the microstructure evolution of strontium barium niobate $Sr_{0.7}Ba_{0.3}Nb_2O_6$ (SBN70) ceramic was examined from a viewpoint of abnormal grain growth generation. The compositions of stoichiometry, $Nb_2O_5$-deficient and $Nb_2O_5$-excess SBN70 were prepared and sintered in the temperature range of 1250–1400 °C for 2 h. The sample with $Nb_2O_5$-excess composition showed a duplex microstructure with abnormally large grains and fine grains, while the $Nb_2O_5$-deficient sample showed a homogeneous and fine-grained microstructure. X-ray diffraction analysis of the $Nb_2O_5$-excess and $Nb_2O_5$-deficient compositions revealed second phases of $Ba_3Nb_{10}O_{28}$ s.s. ($B_3N_5$) and $Sr_2Nb_2O_7$ s.s. ($S_2N$), respectively. Because the $B_3N_5$ phase has a low melting point of 1320 °C, it is believed that the abnormal grain growth generated in the $Nb_2O_5$-excess composition originates from the inhomogeneous distribution of the $B_3N_5$ liquid phase. These second phases also influence the dielectric characteristics of ceramics such as the Curie temperature, the maximum dielectric constant and diffuse phase transition behavior. 

*Keywords:* Dielectric properties; Grain growth; Microstructure-final; SBN; (Sr; Ba) $Nb_2O_6$; Tungsten bronze

## 1. Introduction

$Sr_xBa_{1-x}Nb_2O_6$ (SBN, where $0.25 \leqslant x \leqslant 0.75$) ceramics are ferroelectric materials with tungsten bronze structures, which have excellent electro-optic,[1–3] pyroelectric,[4–6] photorefractive,[7–9] and piezoelectric[3] properties. Even though single crystal SBN has superior properties to polycrystalline SBN, high costs and the difficult fabrication process of a single crystal have limited its application. Therefore, the achievement of full densification with a uniform microstructure of polycrystalline SBN ceramics is greatly desired, which is advantageous with respect to cost and the easier fabrication process. In particular, for optical applications, SBN ceramics should have near theoretical densities. However, considerable difficulties in sintering highly-dense SBN ceramics have been reported and abnormal grain growth often occurs during sintering, which is assumed to be due to the formation of a liquid phase caused by local compositional deviation from stoichiometry.[10–14]

Takahashi et al.[10] proposed that abnormal grain growth in SBN ceramics is due to a small amount of liquid phase which forms due to an incomplete reaction during calcination. Lee et al.[12,13] reported the composition of the liquid phase at the grain boundary of stoichiometric SBN being Nb-rich but Ba-deficient. On the other hand, Fang et al.[14] asserted that the second phase of $SrNb_2O_6$, which is the origin of the abnormal grain growth, decomposed from stoichiometric SBN during ball milling after calcinations. Even though different opinions have been proposed in the literature on the generation of abnormal grain growth in SBN ceramics, there is common agreement that the abnormal grain growth is caused by the Nb-rich liquid phase. However,

* Corresponding author. Tel.: +82-53-950-5635; fax: +82-53-950-5645.
*E-mail address:* jjkim@knu.ac.kr (J.-J. Kim).

0955-2219/02/$ - see front matter 
PII: S0955-2219(02)00025-0

there is still no accepted mechanism to explain the origin of extraordinary microstructure development, such as abnormal grain growth and duplex structures in SBN ceramics.

In this study, therefore, the effect of $Nb_2O_5$ content on the microstructural evolution in tungsten bronze structured $Sr_{0.7}Ba_{0.3}Nb_2O_6$ ceramics was examined. Dielectric properties of the ferroelectric SBN70 were also investigated. The experimental phenomena on the generation of abnormal grain growth and resultant change in dielectric characteristics of the samples are explained and discussed in terms of the second phases produced.

## 2. Experimental

Samples of $Sr_{0.7}Ba_{0.3}Nb_2O_6$ (SBN70) were prepared from the raw materials $BaCO_3$(99.6%), $SrCO_3$(99.4%), and $Nb_2O_5$(99.9%), which have mean particle sizes of 1.40, 1.40 and 0.83 μm, respectively. Different compositions of stoichiometric SBN70, $x$ mol% $Nb_2O_5$-excess SBN70 and $x$ mol% $Nb_2O_5$-deficient SBN70 were prepared using the mixed oxide route, where $x=1$, 3, 5. The compositions are denoted as SBN70 and SBN70$\pm x$ hereafter. The weighed powders were wet mixed for 24 h in a plastic jar with zirconia balls and ethanol.

After drying in an oven, the powders were calcined at 1300 °C for 6 h, then ball milled again for 24 h for crushing. 5 wt.% of aqueous PVA solution was mixed with the powders and sieved to form granules. Green pellets of 10 mm diameter were cold isostatically pressed at a pressure of 100 MPa. Binder burnout of the pellets was carried out at 600 °C for 4 h in air. Samples were sintered at temperatures in the range of 1250–1400 °C for 2 h with a heating rate of 5 °C/min.

Shrinkage and the shrinkage rate of samples during heating were measured using a vertical-loading dilatometer (Rigaku Thermoflex, TMA 8140). X-ray diffraction (XRD; Mac Science, M03XHF) studies were conducted on the sintered specimens to identify the phases. The densities of the sintered samples were measured using an immersion technique. For the microstructural observation of the samples, surfaces were polished and thermally etched. A scanning electron microscopy (SEM; Jeol, JSM-5400) was used for the microstructure observation. Grain sizes of sintered samples were determined using a linear intercept method.[15] SEM micrographs were taken in randomly selected areas of each specimen. Ag electrodes were screen-printed on both surfaces of the sintered samples and fired at 600 °C for 10 min. Dielectric properties were analyzed by an impedance gain phase analyzer (HP4194A) with a frequency swept in steps from 1 kHz to 1 MHz as a function of temperature from −80 to 350 °C in 2 °C increment.

## 3. Results and discussion

### 3.1. Microstructure evolution

Fig. 1 shows the densification behavior of shrinkage and the shrinkage rate of the samples as a function of $Nb_2O_5$ content. The densification behavior of the samples was clearly influenced by the $Nb_2O_5$ content. Most of the densification for the stoichiometric and $Nb_2O_5$ deficient samples occurred in the high sintering temperature range of 1360–1400 °C. A small amount of excess $Nb_2O_5$ significantly enhanced densification at the relatively low sintering temperature of 1320 °C; another shrinkage peak around 1370 °C was also observed. The first shrinkage around 1320 °C is believed to have been due to a liquid phase, which accelerates densification at low temperatures. Another peak in densification at around 1370 °C also occurred between solid grains as observed in the stoichiometric and $Nb_2O_5$-deficient samples. The phase diagram[16] of SBN ceramics also supports the formation of a liquid phase above 1320 °C.

Fig. 2 shows the bulk density of samples as functions of sintering temperature and $Nb_2O_5$ content. The samples were sintered at individual temperatures for 2 h.

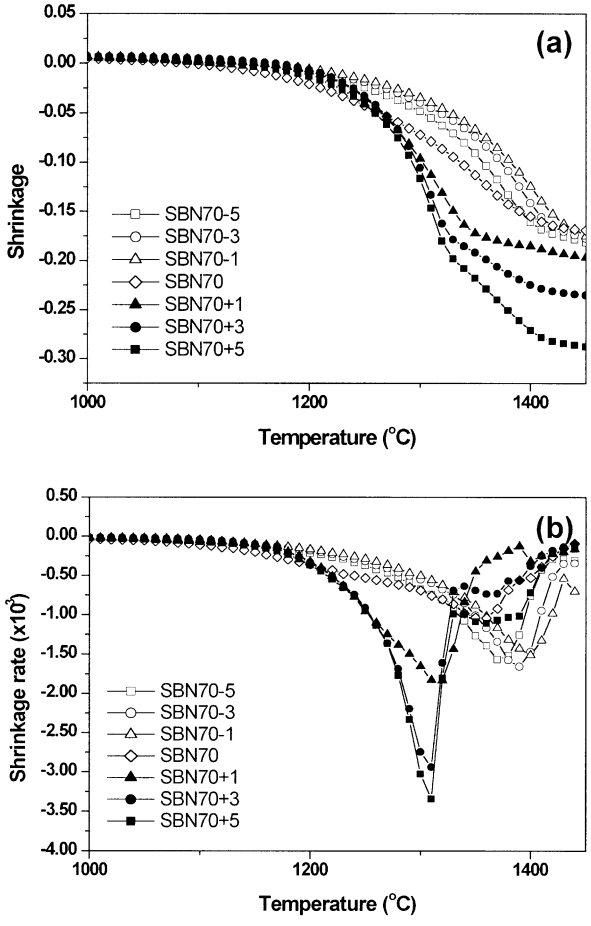


Fig. 1. Densification behavior of samples: (a) shrinkage and (b) shrinkage rate.

In the low sintering temperature region of 1250–1300 °C, the density of the samples with excess $Nb_2O_5$ was higher than that of the $Nb_2O_5$-deficient samples. However in the high sintering temperature region of 1350–1400 °C, the density was lower than that of the $Nb_2O_5$-deficient samples.

Fig. 3 shows the microstructures of samples as functions of $Nb_2O_5$ content and sintering temperature.

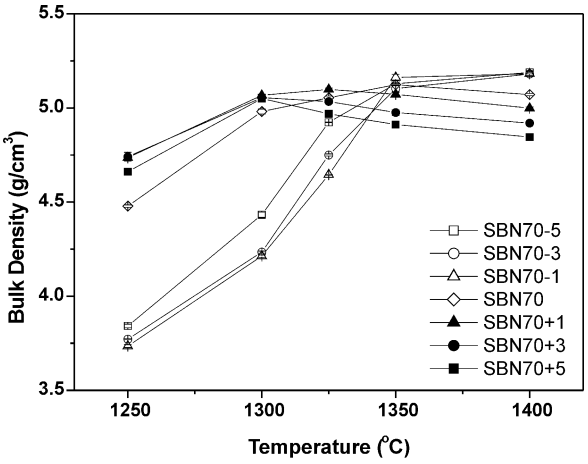


Fig. 2. Bulk densities of samples as functions of $Nb_2O_5$ content and sintering temperature.

When samples with different $Nb_2O_5$ content were sintered at 1300 °C [Fig. 3 (a)–(c)], the bulk densities of the samples were 89.9±0.1, 96.0±0.2 and 96.2±0.2% for SBN70–5, SBN70 and SBN70+5, respectively. The respective grain sizes were 2.8, 5.7 and 4.9 μm. These results show a deficiency of $Nb_2O_5$ retards densification and grain growth. When the samples were sintered at 1325 °C, densification improved to 93.7±0.02 and 96.2±0.2% for SBN70–5 and SBN70, respectively, while little grain growth occurred. However, in the case of SBN70+5, the density decreased to 94.6±0.1% and a duplex microstructure with small grains less than 3 μm and abnormally large grains in the range of 30–40 μm coexisted. The sample shrinkage with respect to the sintering temperature shown in Fig. 1 supports the formation of a liquid phase above 1320 °C in the samples containing excess $Nb_2O_5$. Among the samples of Fig. 3(d)–(f), which were sintered at 1325 °C, abnormal grain growth was observed in SBN70+5. Therefore, it is believed that the excess $Nb_2O_5$ provided the source of the liquid phase, which is the origin of the abnormal grain growth in SBN ceramics. Because abnormal grain growth frequently yields pore isolation, pore agglomeration and crack generation,[17,18] the decreased density in the SBN70+5 is believed to be related to abnormal grain growth. On the other hand, when the sintering

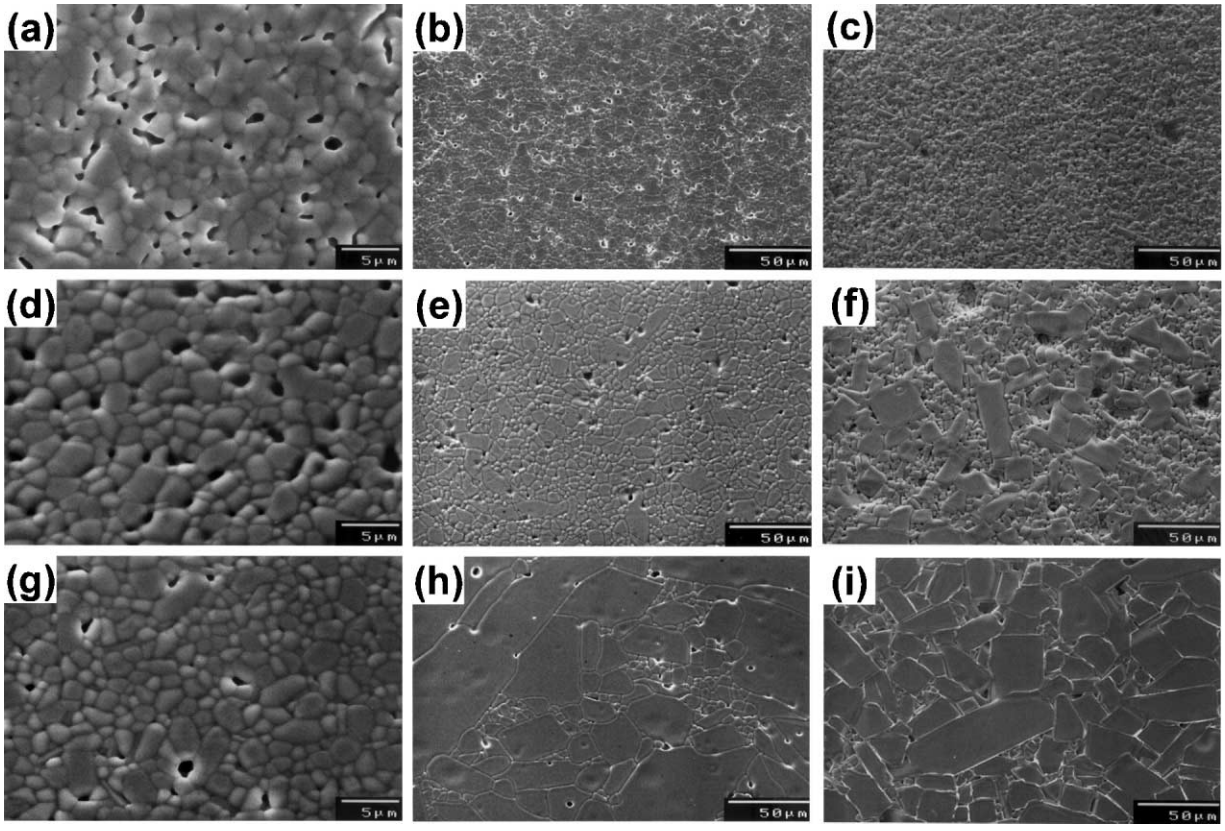


Fig. 3. SEM photographs of SBN70–5 (a, d, g), SBN70 (b, e, h) and SBN70+5 (c, f, i) samples sintered at different sintering temperatures of 1300 °C (a, b, c), 1325 °C (d, e, f) and 1350 °C (g, h, i) for 2 h.

temperature was elevated to 1350 °C, the duplex microstructure disappeared; instead, a large but much more homogeneous distribution of grain size was observed in SBN70 + 5, as shown in Fig. 3(i). When the sintering temperature was elevated, the volume of the liquid phase increased. Because the liquid phase provides the origin of abnormal grain growth in SBN ceramics, it is believed that an increased volume of the liquid phase produces many nucleation sites for abnormal grain growth at once, which then finally led to a homogeneous microstructure distribution.[19,20] However, severe abnormal grain growth was observed in the SBN70 stoichiometric composition (h). The origin of the abnormal grain growth in stoichiometric SBN ceramics has been reported to be the inhomogeneous distribution of the Nb-rich liquid phase.[10–14] Lee et al.[12] proposed that a liquid phase is the origin of localized abnormal grain growth in SBN ceramics. They observed a liquid phase by using a TEM and reported the composition of the liquid phase being Nb-rich but Ba-deficient. They further suggested that the origin of the liquid phase resulted from locally inhomogeneous compositions due to a partially uncompleted calcination process. Further studies on the effect of excess BaO and deficiency of $Nb_2O_5$ on sintering behavior and microstructural development provided evidence for the existence of a liquid phase which assists abnormal grain growth.[13] Takahashi et al.[10] proposed the reason of the abnormal grain growth that the small amount of liquid phase, which was formed due to an incomplete reaction during calcination is the reason of the abnormal grain growth. On the other hand, Fang et al.[14] asserted that the $SrNb_2O_6$ second phase is decomposed from SBN during ball milling after calcination and the second phase is the origin of the abnormal grain growth. Even though different authors have different opinions on the generation of abnormal grain growth, there is a common point in that abnormal grain growth is caused by the Nb-rich liquid phase.

Fig. 4 shows the powder X-ray diffraction spectra of the samples with 5 mol% $Nb_2O_5$-deficient, stoichiometry and 5 mol% $Nb_2O_5$-excess sintered at 1350 °C for 2 h. Fig. 4(a) shows a typical diffraction spectrum for SBN ceramics. However, a magnified view of a selected diffraction range shows traces of second phases $Sr_2Nb_2O_7$ s.s. ($S_2N$) and $Ba_3Nb_{10}O_{28}$ s.s. ($B_3N_5$) in 5 mol% $Nb_2O_5$-deficient and 5 mol% $Nb_2O_5$-excess samples, respectively. As seen in the microstructure Fig. 3(i), when 5 mol% excess $Nb_2O_5$ is added, a second phase was observed along grain boundaries. The EDX line scanning across the grain boundary shows that the second phase is a Ba- and Nb-rich phase, as expected from the phase diagram of the 25% BaO isopleth as a function of $Nb_2O_5$. However, a second phase in the 5 mol% $Nb_2O_5$-deficient samples was not observed in the microstructure. This might be due to the small amount of the second phase with a similar morphology to the matrix. According to the phase diagram,[16] $S_2N$ has a eutectic temperature of > 1420 °C, while that of the $B_3N_5$ phase is around 1320 °C. Therefore, when the $Nb_2O_5$-excess sample is sintered around or over 1320 °C, the second phase of $B_3N_5$ will form a liquid phase, which seems to play a major role in abnormal grain growth in the system.

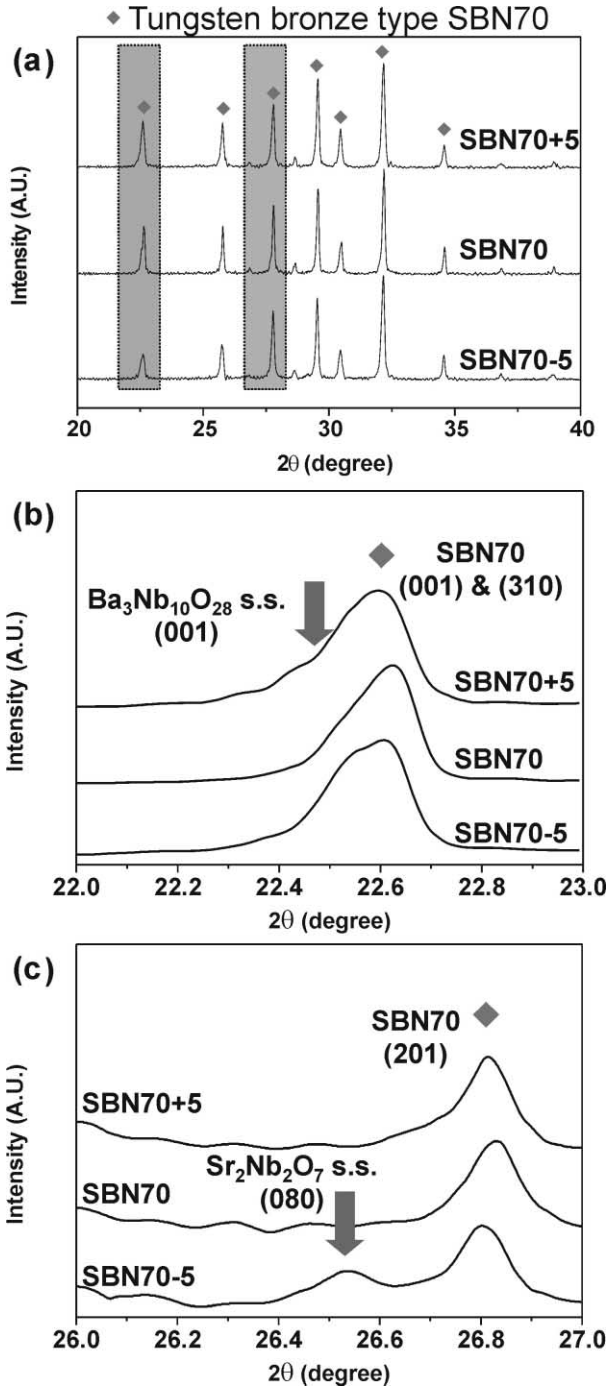


Fig. 4. Powder X-ray diffraction patterns of SBN70–5, SBN70 and SBN70 + 5 specimens sintered at 1350 °C for 2 h.

### 3.2. Dielectric characteristics

Fig. 5 shows the temperature dependence of the dielectric constant and dielectric loss in a range of frequencies for samples with different $Nb_2O_5$ content. The dielectric characteristics show diffuse phase transition (DPT) phenomena (i.e., they exhibit a broad Curie peak in the phase transition range). The positions of the maxima in the dielectric constant (and loss factor) curves versus temperature are frequency dependent and are shifted toward higher temperatures as the frequency increases. SBN ceramics are well-known DPT relaxor materials.[21,22]

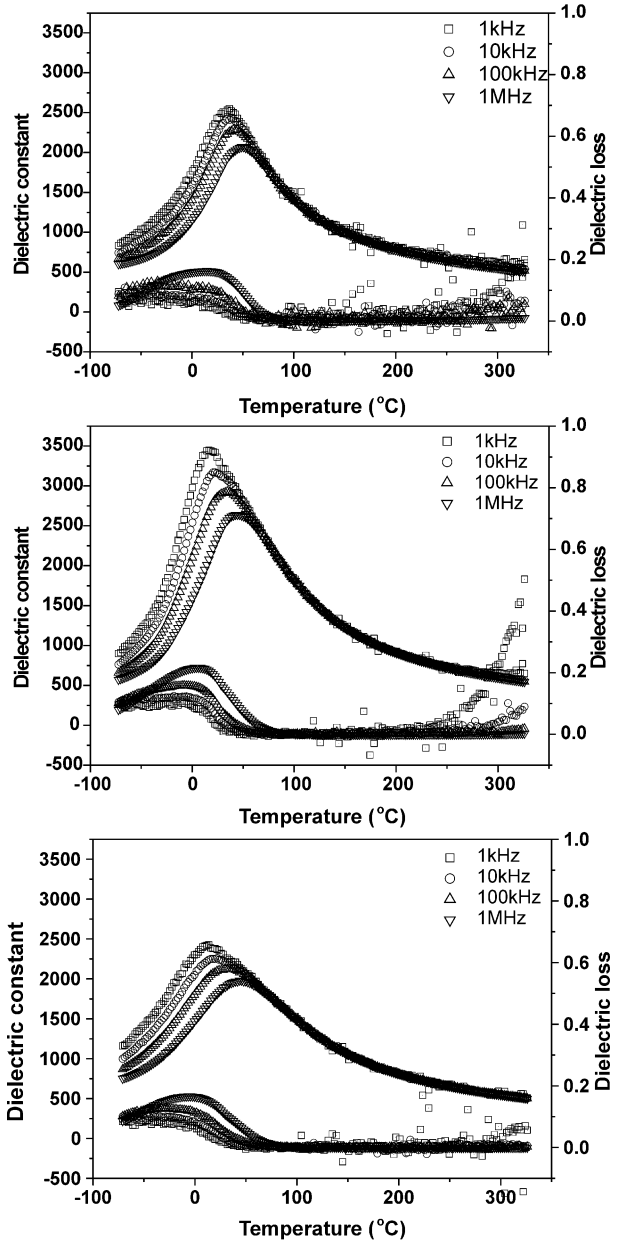


Fig. 5. Temperature dependence of dielectric constant and dielectric loss for (a) SBN70–5 (b) SBN70 and (c) SBN70 + 5 sintered at 1350 °C for 2 h.

Fig. 6(a) shows the maximum dielectric constant of the samples sintered at 1350 °C for 2 h as functions of $Nb_2O_5$ content and measurement frequency. The maximum dielectric constants show the highest value at the stoichiometry composition and decreased as the composition went away from the stoichiometry. This is believed to be due to the second phases in the matrix. Because the dielectric constant of the $Sr_2Nb_2O_7$ is below 100 at the temperature range measured,[23] the second phase of $Sr_2Nb_2O_7$ s.s. seems to have a lower dielectric constant than the ferroelectric matrix. Even a specific dielectric constant of the $Ba_3Nb_{10}O_{28}$ s.s. phase could not present here, though, the decreased dielectric constant in the $Nb_2O_5$-excess sample implies that the $Ba_3Nb_{10}O_{28}$ s.s. phase has a lower dielectric constant than the matrix. Based on this assumption, because the second phase of $B_3N_5$ forms a liquid phase during sintering due to its low melting point, the non-ferroelectric liquid phase at the grain boundaries surrounds the ferroelectric grains as seen in Fig. 3(i). Therefore, the dielectric constant degraded more in the $Nb_2O_5$-excess samples than in the $Nb_2O_5$-deficient samples in which

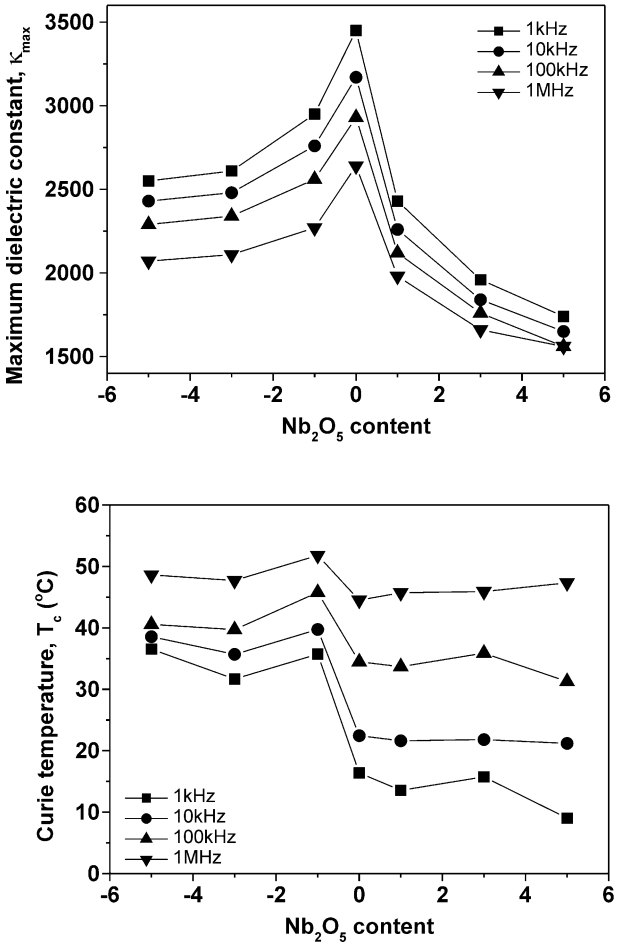


Fig. 6. Variations of (a) maximum dielectric constant and (b) the Curie temperature of samples sintered at 1350 °C for 2 h as function of $Nb_2O_5$ content and frequency.

the second phase of $S_2N$ solid grains are scattered in the matrix. Fig. 6(b) shows the Curie temperatures of the samples derived from dielectric constant curves as functions of $Nb_2O_5$ content and measurement frequency. Note that the Curie temperatures of the samples in $Nb_2O_5$-deficient area are higher than in the $Nb_2O_5$-excess area. The shift of the Curie temperatures implies a change in the Sr/Ba ratio of the matrix. Hence, it is necessary to confirm the composition change of the matrix due to the formation of second phases. The second phase of $B_3N_5$ formed in the $Nb_2O_5$-excess area that contains Ba, while the second phase of $S_2N$ formed in the $Nb_2O_5$-deficient area that contains Sr. This naturally affects the Sr/Ba ratio of the matrix, which is directly connected to the Curie temperature; in other words, the lower the Sr/Ba ratio, the higher the Curie temperature.[4,24] The difference of the Curie temperature ($\Delta T_c$) at different frequencies, for example 1 kHz and 1 MHz, indicates the frequency dependence of the Curie temperature.[25] According to the measured data in Fig. 6(b), $\Delta T_c$ for the $Nb_2O_5$-deficient, stoichiometry and $Nb_2O_5$-excess compositions show 12, 28 and 38 °C, respectively, which suggests that the $Nb_2O_5$-excess sample shows more diffused phase transition as revealed in Fig. 5. It is reported that the degree of DPT increases when the Sr/Ba ratio increased.[4,24,26] From this point of view, therefore, the greater DPT phenomena in the $Nb_2O_5$ excess composition probably reflects the formation of a $Ba_3Nb_{10}O_{28}$ second phase, which increased the Sr/Ba ratio of the matrix. On the other hand, the connectivity between the ferroelectric and non-ferroelectric phases in a sample composed of ferroelectric and non-ferroelectric mixtures might play a role in dielectric behavior.[27]

## 4. Conclusions

Excess $Nb_2O_5$ in SBN ceramics promotes densification at low sintering temperatures. However, when samples are sintered above 1320 °C, which is the eutectic temperature of a Nb-excess liquid phase, abnormal grain growth is generated. In $Nb_2O_5$-deficient samples, homogeneous, small grains were observed in the high density microstructure, even when they were sintered at high sintering temperatures. Second phases of $Ba_3Nb_{10}O_{28}$ and $Sr_2Nb_2O_7$ were found in the $Nb_2O_5$-excess and $Nb_2O_5$-deficient samples, respectively. Since the second phase of $Ba_3Nb_{10}O_{28}$ transforms into a liquid phase during sintering, it is believed that the excess $Nb_2O_5$ is the reason for the abnormal grain growth in SBN ceramics. The second phases of $Ba_3Nb_{10}O_{28}$ and $Sr_2Nb_2O_7$ also changed the Sr/Ba ratio of the matrix. It was found that the Curie temperature shifted and the dielectric constants, as well as DPT behavior, were influenced accordingly.

## Acknowledgements

This work was supported by grant No. R01–2000–00233 from the Basic Research Program of the Korea Science & Engineering Foundation.

## References

1. Jamieson, P. B., Abrahams, S. C. and Bernstein, J. L., Ferroelectric tungsten bronze-type crystal structures. I. Barium strontium niobate $Ba_{0.27}Sr_{0.75}Nb_2O_{5.78}$. *J. Chem. Phys*., 1968, **48**, 5048–5057.
2. Lenzo, P. V., Spencer, E. G. and Ballman, A. A., Electro-optic coefficients of ferroelectrics strontium barium niobate. *Appl. Phys. Lett*., 1967, **11**, 23–24.
3. Nagata, K., Yamamoto, Y., Igarashi, H. and Okazaki, K., Properties of the hot-pressed strontium barium niobate ceramics. *Ferroelectrics*, 1981, **38**, 853–856.
4. Glass, A. M., Investigation of the electrical properties of $Sr_{1-x}Ba_xNb_2O_6$ with special Reference to pyroelectric detection. *J. Appl. Phys*., 1969, **40**, 4699–4713.
5. Lee, S. I. and Choo, W. K., Modified ferroelectric high density strontium barium niobate ceramics for pyroelectric applications. *Ferroelectrics*, 1988, **87**, 209–212.
6. Glass, A. M., Ferroelectric $Sr_{1-x}Ba_xNb_2O_6$ as a fast and sensitive detector of infrared radiation. *Appl. Phys. Lett*., 1968, **13**, 147–149.
7. Imai, T., Yagi, S., Yamazaki, K. and Ono, M., Effects of heat treatment on photorefractive sensitivity of Ce- and Eu-doped strontium barium niobate. *Jpn. J. Appl. Phys*., 1999, **38**, 1984–1988.
8. Venturini, E. L., Spencer, E. G., Lenzo, P. V. and Ballman, A. A., Refractive indices of strontium barium niobate. *J. Appl. Phys*., 1968, **39**, 343–344.
9. Ewbank, M. D., Neugaonkar, R. R., Cory, W. K. and Feinberg, J., Photorefractive properties of strontium-barium niobate. *J. Appl. Phys*., 1987, **62**, 374–380.
10. Takahashi, J., Nishiwaki, S. and Kodaira, K., Sintering and microstructure for $Sr_{0.6}Ba_{0.4}Nb_2O_6$ ceramics. *Ceram. Trans*., 1994, **41**, 363–370.
11. Nishiwaki, S., Takahashi, J. and Kodaira, K., Effect of additives on microstructure development and ferroelectric properties of $Sr_{0.3}Ba_{0.7}Nb_2O_6$ ceramics. *Jpn. J. Appl. Phys*., 1994, **33**, 5477–5481.
12. Lee, H. Y. and Freer, R., The mechanism of abnormal grain growth in $Sr_{0.6}Ba_{0.4}Nb_2O_6$ ceramics. *J. Appl. Phys*., 1997, **81**, 376–382.
13. Lee, H. Y. and Freer, R., Abnormal grain growth and liquid-phase sintering in $Sr_{0.6}Ba_{0.4}Nb_2O_6$ (SBN40) ceramics. *J. Mat. Sci*., 1998, **33**, 1703–1708.
14. Fang, T. T., Chen, E. and Lee, W. J., On the discontinuous grain growth of $Sr_xBa_{1-x}Nb_2O_6$ ceramics. *J. Eur. Ceram. Soc*., 2000, **20**, 527–530.
15. Fullmann, R. L., Measurement of particle size on opaque bodies. *Trans. AIME*, 1953, **3**, 447–452.
16. Carruthers, J. R. and Grasso, M., Phase Equilibria in the Ternary System BaO-SrO-$Nb_2O_5$. *J. Electrochem. Soc*., 1970, **117**, 1426–1430.
17. Shin, S. D., Sone, C. S., Han, J. H. and Kim, D. Y., Effect of sintering atmosphere on the densification and abnormal grain growth of ZnO. *J. Am. Ceram. Soc*., 1996, **79**, 565–567.
18. Greskovich, C., Preparation of high-density $Si_3N_4$ by a gas-pressure sintering process. *J. Am. Ceram. Soc*., 1981, **64**, 725–730.
19. Wong, J., Sintering and varister characteristics of ZnO-$Bi_2O_3$ ceramics. *J. Appl. Phys*., 1980, **51**, 4453.

20. Hennings, D. F., Control of liquid phase discontinuous grain growth in barium titanate. *J. Am. Ceram. Soc.*, 1987, **70**, 23–27.
21. Cross, L. E., Relaxor ferroelectrics. *Ferroelectrics*, 1987, **76**, 241–267.
22. Cross, L. E., Relaxor ferroelectrics: an overview. *Ferroelectrics*, 1994, **151**, 305–320.
23. Madelung, O., *Landolt-Börnstein. Ferroelectric and Related Substances (Fig. 619)*. Springer-Verlag, Berlin, 1990.
24. VanDamme, N. S., Sutherland, A. E., Jones, L., Bridger, K. and Winzer, S. R., Fabrication of optically transparent and electro-optic strontium barium niobate ceramics. *J. Am. Ceram. Soc.*, 1991, **74**, 1785–1792.
25. Butcher, S. J. and Thomas, N. W., Ferroelectricity in the system $Pb_{1-x}Ba_x(Mg_{1/3}Nb_{2/3})O_3$. *J. Phys. Chem. Solids*, 1991, **52**, 595–600.
26. Viehland, D., Xu, Z. and Huang, W. H., Structure-property relationships in strontium barium niobate I. Needle-like nanopolar domains and the metastably-locked incommensurate structure. *Philosophical Magazine A*, 1995, **71**, 205–217.
27. Sohn, J. H., Cho, J. W., Lee, J. H. and Cho, S. H., Strong ferroelectric perovskite phase in Pb-containing composites. *Solid State Ionics*, 1998, **108**, 141–149.